Inorganic Chemistry

Article

pubs.acs.org/IC

# Shuttling of Nickel Oxidation States in $N_4S_2$ Coordination Geometry versus Donor Strength of Tridentate $N_2S$ Donor Ligands

Sudip K. Chatterjee,[†] Suprakash Roy,[†] Suman Kumar Barman,[‡] Ram Chandra Maji,[†] Marilyn M. Olmstead,[§] and Apurba K. Patra*[,†]

[†]Department of Chemistry, National Institute of Technology Durgapur, Mahatma Gandhi Avenue, Durgapur 713 209, India

[‡]Department of Chemistry, Indian Institute of Technology Kanpur, Kanpur 208 016, India

[§]Department of Chemistry, University of California, Davis, California 95616, United States

Supporting Information

**ABSTRACT:** Seven bis-$Ni^{II}$ complexes of a $N_2S$ donor set ligand have been synthesized and examined for their ability to stabilize $Ni^0$, $Ni^I$, $Ni^{II}$ and $Ni^{III}$ oxidation states. Compounds **1**−**5** consist of modifications of the pyridine ring of the tridentate Schiff base ligand, 2-pyridyl-N-(2′-methylthiophenyl)methyleneimine ($^X$L1), where X = 6-H, 6-Me, 6-*p*-ClPh, 6-Br, 5-Br; compound **6** is the reduced amine form (L2); compound **7** is the amide analog (L3). The compounds are perchlorate salts except for **7**, which is neutral. Complexes **1** and **3**−**7** have been structurally characterized. Their coordination geometry is distorted octahedral. In the case of **6**, the tridentate ligand coordinates in a facial manner, whereas the remaining complexes display meridional coordination. Due to substitution of the pyridine ring of $^X$L1, the Ni−$N_{py}$ distances for **1**∼**5** < **3** < **4** increase and UV−vis $\lambda_{max}$ values corresponding to the $^3A_{2g}(F)\rightarrow{}^3T_{2g}(F)$ transition show an increasing trend **1**∼**5** < **2** < **3** < **4**. Cyclic voltammetry of **1**−**5** reveals two quasi-reversible reduction waves that correspond to $Ni^{II}\rightarrow Ni^I$ and $Ni^I\rightarrow Ni^0$ reduction. The $E_{1/2}$ for the $Ni^{II}/Ni^I$ couple decreases as **1** > **2** > **3** > **4**. Replacement of the central imine N donor in **1** by amine **6** or amide **7** N donors reveals that complex **6** in $CH_3CN$ exhibits an irreversible reductive response at $E_{pc}$ = −1.28 V, $E_{pa}$ = +0.25 V vs saturated calomel electrode (SCE). In contrast, complex **7** shows a reversible oxidation wave at $E_{1/2}$ = +0.84 V ($\Delta E_p$ = 60 mV) that corresponds to $Ni^{II}\rightarrow Ni^{III}$. The electrochemically generated $Ni^{III}$ species, $[(L3)_2Ni^{III}]^+$ is stable, showing a new UV−vis band at 470 nm. EPR measurements have also been carried out.

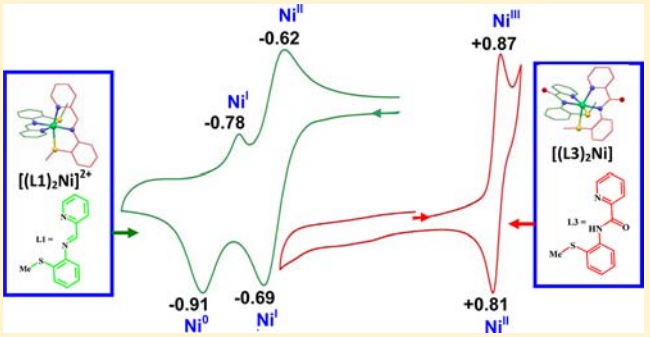


## INTRODUCTION

In nickel-containing enzymes, Ni can be either redox active or inactive, and it is found in $S_x$, $N_xS_y$, or $N_xO_y$ coordination environments.[1] In [Ni−Fe] hydrogenase, Ni oxidation states switch among +1, +2, and +3 during the reversible catalytic oxidation of dihydrogen.[2] Therefore, model complexes for which the stabilization of nickel in both lower and higher than its normal +2 oxidation state required is of interest. Previous work on model complexes of [Ni−Fe]hydrogenase, reported by Mascharak and co-workers,[3] revealed that the mentioned three oxidation states of Ni are highly achievable in imine, pyridine N, and thiolato S ligand donor sets. The strong σ-donor ability of deprotonated amide[4] and oxime[5] ligands has successfully been used to stabilize the higher oxidation states of nickel. For example, the tridentate bis-amide ligand, 2,6-bis[N-(phenyl)-carbamoyl]pyridine, forms $Ni^{II}$, $Ni^{III}$, and $Ni^{IV}$ oxidation states,[4b] and electrosynthesis involving a thioether-azo-oxime ligand[5c] yields a series of $Ni^{III}N_4S_2$ complexes. On the other hand, the common softer donor atoms such as N of imine, S of thioether/thiol, and P of phosphene have a σ-donor and a π-acceptor property that stabilizes the $Ni^I$ state. Several examples of $Ni^{II}$ complexes with ligands containing such soft donor atoms are known where the formation of a $Ni^I$ species is evident by chemical or electrochemical reduction.[3,6] However, the main challenges are the tendency of the generated $Ni^I$ species to disproportionate back to the $Ni^{II}$ and $Ni^0$ states[5a,b] and the formation of the $Ni^{II}$-ligand anion radical[7] species where the ligand system is more prone to be reduced than the metal.

Alkyl amine N are σ-donors, with no π-accepting properties, and hence are not a good choice for stabilizating the $Ni^I$ state (high cathodic potential needed for $Ni^{II}\rightarrow Ni^I$ reduction).[8] However, it has been noted that amine-N methylation anodically shifts the reduction potential and also appreciably increases the stability of electrochemically generated $Ni^I$ species.[9] Thus, the ease of Ni's oxidation state flipping and its characteristic chemical/biological reactivity is strongly influenced by the nature and number of various types of donor atoms. For a clear understanding of the effect of a

**Received:** March 22, 2012
**Published:** June 29, 2012

   dx.doi.org/10.1021/ic300606g | *Inorg. Chem.* 2012, 51, 7625−7635

particular type of donor atom, it is desirable to vary the strength of one donor atom while keeping the remaining donors fixed and to examine the redox and spectral properties of these complexes.

Series of $NiN_4S_2$ chromophores with common ligand architectures are rare. To the best of our knowledge, Chakravorty et al. have reported one such family of $Ni^{III}N_4S_2$ chromophores, stabilized in thioether-azo-oxime ligand environment.[5c] In most of the $NiN_4S_2$ chromophores, the S ligation comes from thiosemicarbazone and its derivatives,[10] and fewer examples of either thiol[3a] or thioether[4a,5c,6g,h,11] S linkages to Ni in combination with imine or amine or amide N donors are known. Herein, we report the synthesis, structure, and electrochemical and spectral properties of a series of $Ni^{II}N_4S_2$ complexes. To vary the pyridine (py) N donor strength; different *ortho* substituents on the pyridine ring, possessing +I/−I inductive effects have been chosen. To probe the effect of the middle N donor strength of the tridentate ligands the imine, amine, and amide functional groups have been incorporated in the ligand framework (Scheme 1). Redox and spectral

**Scheme 1. Structural Representations of the Ligands**

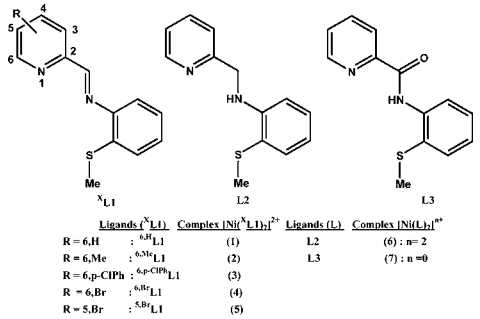


properties of these complexes clearly revealed that the pyridine, imine N, and thioether S donor set may be able to stabilize the $Ni^{I}$ state. The electron withdrawing substituent (e.g., −Br) near the pyridine N donor decreases its donor strength and shifts the $Ni^{II}\rightarrow Ni^{I}$ reduction potential by 200 mV more anodic than the unsubstituted one. It is also reported that the amide N, even with the thioether S donor, can stabilize the $Ni^{III}$ state, whereas the amine N and thioether S together only favor the $Ni^{II}$ state.

## EXPERIMENTAL SECTION

**Materials and Reagents.** Pyridine-2-carboxaldehyde, pyridine-2-carboxylic acid, 2-(methylthio)aniline, triphenylphosphite, sodium hydride, $[Ni(H_2O)_6](ClO_4)_2$, sodium borohydride, 6-bromo-pyridine-2-aldehyde, 6-methyl-pyridine-2-aldehyde, 6-*p*-chlorophenyl-pyridine-2-aldehyde, 5-bromo-pyridine-2-aldehyde, sodium perchlorate ($NaClO_4$) were purchased from Aldrich Chemical Co. and used without further purification. $CH_3CN$, $CH_3OH$, $C_2H_5OH$, $CHCl_3$, pyridine (py), and diethyl ether $(C_2H_5)_2O$ used either for spectroscopic studies or for syntheses were purified and dried following standard procedures prior to use.

**Synthesis Safety Note.** Transition metal perchlorates should be handled cautiously as these are hazardous and explosive upon heating. No such happening is encountered in the present study.

**General Method of Schiff Base Ligand Syntheses.** To a stirred solution of pyridine-2-carboxaldehyde or of its substituted derivative in freshly distilled methanol or toluene was added a methanol/toluene solution of 2-(methylthioaniline). The reaction mixture was then refluxed under nitrogen for 6 h. After cooling the reaction mixture to room temperature, the solvent was removed completely using a rotary evaporator to yield a thick yellow oil. The oil was then dissolved in $CHCl_3$ and successively washed with distilled water, brine solution, and finally distilled water. The organic layer separated out was then dried over $Na_2SO_4$ for 1 h and filtered, and the solvent was completely removed. The yellow oil kept at 4 °C overnight to get a yellow solid. The solid was then recrystallized from diethyl ether that afforded crystals of the respective Schiff base ligands.

**2-Pyridyl-N-(2′-methylthiophenyl)methyleneimine, L1.** Condensation of 1.0 g of pyridine-2-carboxaldehyde (9.33 mmol) with 1.30 g of 2-(methylthioaniline) (9.33 mmol) in 15 mL $CH_3OH$ yielded 1.80 g of L1 (yield: 84%).[12]

**6-Methyl-2-pyridyl-N-(2′-methylthiophenyl)-methyleneimine, $^{6,Me}$L1.** Condensation of 0.1 g of 6-methyl-pyridine-2-carboxaldehyde (0.82 mmol) with 0.115 g of 2-(methylthioaniline) (0.82 mmol) in 30 mL $CH_3OH$ yielded 0.16 g of $^{6,Me}$L1 (yield: 77%). Elemental analysis calcd for $C_{14}H_{14}N_2S$ ($^{6,Me}$**L1**): C 69.39, H 5.82, N 11.56. Found: C 69.11, H 5.76, N 11.43; Selected IR frequencies (KBr disk, $cm^{-1}$): 3055(w), 2982(w), 2917(w), 1626(vs), 1588(vs), 1572(vs), 1466(vs), 1437(s), 1335(w), 1284(w), 1204(m), 1151(w), 1120(s), 1046(m), 988(m), 970(w), 861(w), 842(w), 803(s), 756(s), 732(s), 683(m), 644(w), 538(w), 521(w), 450(w). $^1$H NMR (300 MHz, $CDCl_3$): $\delta$ 8.55 (1H, s, HC═N), 8.15 (1H, d, pyridine proton), 7.70 (1H, t, pyridine proton), 7.24−7.14 (4H, m, phenyl ring proton), 7.08 (1H, d, pyridine ring proton), 2.62 (3H, s, methyl group adjacent to pyridine N), 2.47 (3H, s, methyl group of S-Me).

**6-*p*-Chlorophenyl-2-pyridyl-N-(2′-methylthiophenyl)-methyleneimine, $^{6,p\text{-}ClPh}$L1.** condensation of 0.50 g of pyridine-2-carboxaldehyde (2.29 mmol) with 0.32 g of 2-(methylthioaniline) (2.29 mmol) in 25 mL toluene yielded 0.71 g of $^{6,p\text{-}ClPh}$L1 (yield: 90%). Elemental analysis calcd for $C_{19}H_{16}N_2SCl$: C 67.15, H 4.75, N 8.24. Found: C 67.04, H 4.65, N 8.22. Selected IR frequencies (KBr disk, $cm^{-1}$): 3059(w), 2963(s), 2916(w), 1629(vs), 1588(vs), 1575(vs), 1466(s), 1450(vs), 1336(w), 1262(vs), 1205(m), 1181(m), 1037(w), 989(w), 972(w), 897(vw), 846(w), 803(m), 742(m), 696(m), 642(w), 571(vw), 554(vw), 450(vw). $^1$H NMR (300 MHz, $CDCl_3$): $\delta$ 8.65 (1H, s, HC═N), 8.29 (1H, d, pyridine proton), 8.01 (2H, d, pyridine/*p*-ClPh proton), 7.88 (1H, t, pyridine ring proton), 7.78 (1H, d, *p*-ClPh proton), 7.47 (2H, d, *p*-ClPh proton), 7.25−7.10 (4H, m, phenyl ring proton), 2.49 (3H, s, methyl group of S-Me).

**6-Bromo-2-pyridyl-N-(2′-methylthiophenyl)-methyleneimine, $^{6,Br}$L1.** Condensation of 0.15 g of 6-bromo-pyridine-2-carboxaldehyde (0.806 mmol) with 0.112 g of 2-(methylthioaniline) (0.804 mmol) in 10 mL $CH_3OH$ yielded 0.21 g of $^{6,Br}$L1 (yield: 85%). Elemental analysis calcd for $C_{13}H_{11}N_2SBr$ ($^{6,Br}$L1): C 50.82, H 3.61, N 9.12. Found: C 50.38, H 3.57, N 9.01. Selected IR frequencies (KBr disk, $cm^{-1}$): 3067(w), 2981(w), 2917(w), 2858(vw), 1624(vs), 1576(s), 1555(s), 1465(m), 1436(s), 1337(w), 1265(w), 1202(w), 1156(m), 1122(m), 1077(m), 984(m), 975(w), 896(m), 841(w), 804(s), 761(s), 731(vs), 708(w), 673(w), 637(w), 548(w), 505(w), 452(w), 436(w). $^1$H NMR (300 MHz, $CDCl_3$): $\delta$ 8.53 (1H, s, HC═N), 8.31 (1H, d, pyridine proton), 7.67−7.96 (1H, m, pyridine proton), 7.58 (1H, d, pyridine proton), 7.28−7.07 (4H, m, phenyl ring proton), 2.48 (3H, s, methyl group of S-Me).

**5-Bromo-2-pyridyl-N-(2′-methylthiophenyl)-methyleneimine, $^{5,Br}$L1.** Condensation of 0.1 g of 5-bromo-pyridine-2-carboxaldehyde (0.53 mmol) with 0.075 g of 2-(methylthioaniline) (0.53 mmol) in 10 mL $CH_3OH$ yielded 0.122 g of $^{5,Br}$L1 (yield: 75%). Elemental analysis calcd for $C_{13}H_{11}N_2SBr$ ($^{5,Br}$L1): C 50.82, H 3.61, N 9.12. Found: C 50.68, H 3.55, N 9.08. Selected IR frequencies (KBr disk, $cm^{-1}$): 3056(w), 2984(w), 2917(w), 1623(vs), 1570(s), 1471(vs), 1440(s), 1366(m), 1350(m), 1260(m), 1192(w), 1083(s), 1006(s), 957(w), 880(m), 831(s), 757(s), 738(s), 715(m), 666(w), 631(m), 552(w), 492(s), 416(m). $^1$H NMR (300 MHz, $CDCl_3$): $\delta$ 8.77 (1H, s, pyridine proton adjacent to N), 8.53 (1H, s, HC═N), 8.23 (1H, d, pyridine proton), 7.96 (1H, d, pyridine proton), 7.37 (1H, t, pyridine proton), 7.28−7.09 (4H, m, phenyl ring proton), 2.48 (3H, s, methyl group of S-Me).

**2-Pyridyl-N-(2′-methylthiophenyl)methylamine, L2.** In a round-bottom flask, 0.5 g (2.19 mmol) of L1 was dissolved in 30 mL of freshly distilled $CH_3OH$ with development of a light yellow


dx.doi.org/10.1021/ic300606g | *Inorg. Chem.* 2012, 51, 7625−7635

color. The flask was then placed on an ice-water bath. Solid $NaBH_4$ (1.25 g, 33 mmol) was added pinchwise to the vigorously stirred yellow solution of L1. The solution became hazy and the yellow color faded to almost colorless with effervescence of hydrogen. After complete addition of $NaBH_4$, the reaction mixture was heated to 40 °C on a water bath for 30 min and was stirred further at room temperature for 3 h. The solution was again placed in an ice-bath and 30 mL of brine solution was added to it, giving a pale yellowish white precipitate. Methanol was then rotary evaporated, and the reaction mixture was extracted with ether (3 × 30 mL). The yellow ether layer was then washed with distilled water, and finally, it was dried over solid $Na_2SO_4$ and filtered. Solvent removal was yielded 0.39 g of L2 as pale yellow oil (Yield: 77%). Elemental analysis calcd for $C_{13}H_{14}N_2S$ (L2): C 67.79, H 6.13, N 12.16. Found: C 67.71, H 5.96, N 12.11. Selected IR frequencies (KBr disk, $cm^{-1}$): 3358(s, amine-NH), 3066(m), 3012(w), 2920(m), 1588(vs), 1570(vs), 1478(vs), 1448(vs), 1353(w), 1320(s), 1285(m), 1161(m), 1089(w), 1040(s), 994(m), 969(m), 829(vs), 752(vs), 617(w), 464(m), 402(m). $^1H$ NMR (300 MHz, $CDCl_3$): $\delta$ 8.59 (1H, d, pyridine proton adjacent to N), 7.61 (1H, t, pyridine proton), 7.41 (1H, d, pyridine proton), 7.32 (1H, d, phenyl ring proton), 7.09−7.28 (2H, m, phenyl ring proton), 6.65 (1H, t, pyridine ring proton), 6.53 (1H, d, pyridine ring proton), 5.88 (1H, broad s, amine), 4.53 (2H, s, $-CH_2-N$), 2.37 (3H, s, methyl group of S-Me).

**N-2-Methylthiophenyl-2′-pyridinecarboxamide, L3.** To a stirred pyridine solution (10 mL) of picolinic acid (1.0 g, 8.13 mmol) was added dropwise a pyridine solution (2 mL) of 2-(methylthioaniline) (1.13 g, 8.13 mmol). The reaction mixture was stirred at 70 °C in an oil bath for 30 min. To this solution was added triphenylphosphite (2.78 g, 8.13 mmol) dropwise, and the temperature was raised to 110 °C and stirred for 6 h. The pyridine was removed using rotary evaporator, and the light yellow oil thus obtained was kept in the freezer overnight to obtain a white solid. The white solid was washed with distilled water and then dissolved with warm $C_2H_5OH/H_2O$ mixture, slow evaporation of which afforded 1.73 g of white needlelike crystals of **L3** (Yield: 87%). Elemental analysis calcd for $C_{13}H_{12}N_2SO$ (L3): C 63.91, H 4.95, N 11.47. Found: C 63.85, H 4.96, N 11.38. Selected IR frequencies (KBr disk, $cm^{-1}$): 3278(s, amide-NH), 3066(m), 2920(m), 1682(vs), 1592(s), 1578(vs), 1514(vs), 1467(m), 1440(s), 1426(s), 1302(s), 1280(m), 1135(w), 1114(m), 1089(m), 1059(m), 998(m), 977(m), 942(m), 897(m), 814(m), 749(vs), 691(vs), 621(w), 588(m), 468(m), 402(w). $^1H$ NMR (300 MHz, $CDCl_3$): $\delta$ 11.04 (1H, s, amide-NH), 8.68 (1H, d, pyridine ring proton), 8.56 (1H, d, pyridine proton), 8.30 (1H, d, phenyl ring proton), 7.9 (1H, t, pyridine ring proton), 7.52 (2H, m, phenyl protons), 7.34 (1H, t, pyridine ring proton), 7.26 (1H, s, phenyl proton), 2.46 (3H, s, methyl group of S−Me).

**Synthesis of Complexes.** *$[Ni(L1)_2](ClO_4)_2$*, ***1***. To the stirred yellow solution of ligand L1 (50 mg, 0.210 mmol) in 10 mL dry $CH_3CN$ was added dropwise a 5 mL $CH_3CN$ solution of $[Ni(H_2O)_6](ClO_4)_2$ (40 mg, 0.10 mmol). The color of the solution changed to yellowish red and was stirred for 2 h. To this solution was then layered 20 mL of dry diethyl ether and kept at 4 °C temperature overnight. A yellowish red microcrystalline solid precipitated, was filtered, and was washed with ether. The solid was then redissolved in 5 mL $CH_3CN$. Ether diffusion to this solution yielded 68 mg of yellowish red needle-shaped crystals of **1** after two days at −10 °C (Yield: 87%). Elemental analysis calcd for $C_{26}H_{24}N_4O_8S_2Cl_2Ni$, **1**: C 43.72, H 3.39, N 7.84. Found: C 43.68, H 3.30, N 7.79. Selected IR frequencies (KBr disk, $cm^{-1}$): 3071(w), 2963(m), 2926(w), 1596(s), 1483(m), 1443(w), 1370(w), 1310(w), 1261(m),1241(w), 1097-(br,vs), 1019(m), 960(w), 951(w), 803(m), 787(m), 772(m), 742(m), 645(w), 622(m), 504(m), 429(w), 418(w). EI (electron ionization) mass spectrum $m/z$ (%): 257.02 ($M^{2+}/2$, 95) for $[Ni(L1)_2]^{2+}$, 229.06 ($(L1+H)^+$, 100). Absorption spectrum [$\lambda_{max}$, nm ($\varepsilon$, $M^{-1}$ $cm^{-1}$), in MeCN] 234 sh (30290), 246 sh (26160), 318 sh (22170), 333 (23790), 347 sh (21910), 366 sh (13650), 520 sh (170), 803 (46), 940 sh (22).

*$[Ni(^{6,Me}L1)_2](ClO_4)_2$*, ***2***. This compound was prepared similarly (0.59 g, yield 77%) to **1** using 0.05 g of $^{6,Me}$L1 (0.20 mmol) and 0.038 g of $[Ni(H_2O)_6](ClO_4)_2$ (0.10 mmol) in 15 mL of $CH_3CN$. Crystals suitable for X-ray diffraction were grown by diffusion of ether into a concentrated $CH_3CN$ solution of **2** at 4 °C. Elemental analysis calcd for $C_{28}H_{28}N_4O_8S_2Cl_2Ni$, **2**: C 45.34, H 3.78, N 7.55. Found: C 45.24, H 3.71, N 7.49. Selected IR frequencies (KBr disk, $cm^{-1}$): 3081(w), 3009(w), 2923(w), 1595(s), 1478(s), 1463(w), 1382(m), 1254(m), 1235(w), 1089(vs), 1008(m), 955(w), 874(w), 803(m), 777(m), 741(m), 636(m), 624(s), 580(w), 532(m), 474(w). EI mass spectrum $m/z$ (%): 398.87 ($[Ni(^{6,Me}L1)(ClO_4)]^+$, 15) 243.02 ($(^{6,Me}L1+H)^+$, 100). Absorption spectrum [$\lambda_{max}$, nm ($\varepsilon$, $M^{-1}$ $cm^{-1}$), in MeCN] 237 sh (25700), 248 sh (23760), 320 sh (21700), 339 (25140), 354 sh (23420), 372 sh (14130), 870 (40).

*$[Ni(^{6,p\text{-}ClPh}L1)_2](ClO_4)_2$*, ***3***. This compound was prepared similarly (0.38 g, yield 55%), using 0.05 g of $^{6,p\text{-}ClPh}$L1 (0.14 mmol) and 0.027 g of $[Ni(H_2O)_6](ClO_4)_2$ (0.07 mmol) in 15 mL of a mixed solvent of $CH_3CN/CH_2Cl_2$ (4:1 v/v). Crystals suitable for X-ray diffraction were grown from a concentrated $CH_3CN$ solution of **3**, using ether diffusion at 4 °C. Elemental analysis calcd for $C_{38}H_{30}N_4O_8S_2Cl_4Ni$, **3**: C 48.48, H 3.21, N 5.99. Found: C 48.37, H 3.11, N 5.88. Selected IR frequencies (KBr disk, $cm^{-1}$): 3073(m), 3011(w), 2917(w), 1595(s), 1561(m), 1480(s), 1450(s), 1369(m), 1257(w), 1232(m), 1096(vs), 1007(s), 949(w), 846(m), 807(s), 762(s), 750(s), 647(m), 620(s), 571(w), 533(m), 476(m), 425(w). EI mass spectrum $m/z$ (%): 367.85 ($M^{2+}/2$, 100) for $[(^{6,p\text{-}ClPh}L1)_2Ni]^{2+}$, 338.91 ($(^{6,p\text{-}ClPh}L1+H)^+$, 40). Absorption spectrum [$\lambda_{max}$, nm ($\varepsilon$, $M^{-1}$ $cm^{-1}$), in MeCN] 205 sh (66070), 243 (44565), 270 sh (33730), 347 (18400), 382 sh (10530), 880 (42).

*$[Ni(^{6,Br}L1)_2](ClO_4)_2$*, ***4***. This compound was prepared similarly (0.56 g, yield 79%) using 0.05 g of $^{6,Br}$L1 (0.16 mmol), 0.03 g of $[Ni(H_2O)_6](ClO_4)_2$ (0.08 mmol) in 15 mL of $CH_3CN$. Crystals suitable for X-ray diffraction were grown from concentrated $CH_3CN$ solution of **4** using ether diffusion at 4 °C. Elemental analysis calcd for $C_{26}H_{22}N_4O_8S_2Cl_2Br_2Ni$, **4**: C 35.81, H 2.52, N 6.42. Found: C 35.76, H 2.39, N 6.36. Selected IR frequencies (KBr disk, $cm^{-1}$): 3077(m), 3011(w), 2926(m), 1587(s), 1547(s), 1475(s), 1437(s), 1370(m), 1361(w), 1235(m), 1088(br,vs), 1003(m), 956(w), 860(w), 802(m), 769(m), 734(m), 679(w), 624(s), 583(w), 568(w), 530(m), 472(w), 427(w). EI mass spectrum $m/z$ (%): 308.91 ($(^{6,Br}L1+H)^+$, 100). Absorption spectrum [$\lambda_{max}$, nm ($\varepsilon$, $M^{-1}$ $cm^{-1}$), in MeCN] 248 (29125), 264 sh (25550), 293 (18470), 333 (15560), 351 (15910), 370 sh (12700), 890 (30).

*$[Ni(^{5,Br}L1)_2](ClO_4)_2{\cdot}CH_3CN$*, ***5***$\cdot CH_3CN$. This compound was prepared similarly (0.54 g, yield 76%), using 0.05 g of $^{5,Br}$L1 (0.16 mmol) and 0.03 g of $[Ni(H_2O)_6](ClO_4)_2$ (0.08 mmol) in 15 mL of $CH_3CN$. Crystals suitable for X-ray diffraction were grown from a concentrated $CH_3CN$ solution of **5**, using ether diffusion at 4 °C. Elemental analysis calcd for $C_{28}H_{25}N_5O_8S_2Br_2Cl_2Ni$, **5**$\cdot CH_3CN$: C 36.83, H 2.73, N 7.66. Found: C 36.77, H 2.67, N 7.61. Selected IR frequencies (KBr disk, $cm^{-1}$): 3056(w), 3020(m), 2925(m), 2251(w, $\nu_{CN}$ of $CH_3CN$), 1583(m), 1545(s), 1480(s), 1433(m), 1386(w), 1358(m), 1305(w), 1265(w),1232(m), 1092(br,vs), 1031(m), 972(w), 954(w), 916(m), 835(m), 772(s), 744(w), 643(w), 655(w), 624(s), 545(w), 507(m), 472(w), 424(w). EI mass spectrum $m/z$ (%): 335.57 ($M^{2+}/2$, 25) for $[(^{5,Br}L1)_2Ni]^{2+}$, 308.64 ($(^{5,Br}L1+H)^+$, 100). Absorption spectrum [$\lambda_{max}$, nm ($\varepsilon$, $M^{-1}$ $cm^{-1}$), in MeCN] 270 (21770), 330 sh (21460), 342 (23520), 357 (22770), 380 sh (14200), 805 (45).

*$[Ni(L2)_2](ClO_4)_2$*, ***6***. Ligand L2 (0.05 g, 0.217 mmol) was taken in a Schlenk flask, and to it, 7 mL of dry $CH_3CN$ was added. To this pale yellow clear solution was added dropwise a $CH_3CN$ solution (3 mL) of $[Ni(H_2O)_6](ClO_4)_2$ (0.04 g, 0.106 mmol) under nitrogen atmosphere. The color of the solution changed immediately to light brownish yellow, which was allowed to stir for 2 h. Dry ether (25 mL) was layered to this solution and kept at 4 °C. After 3 days, light violet block shaped crystals obtained were filtered, washed with ether and dried under vacuum (0.56 g, yield 72%). Elemental analysis calcd for $C_{26}H_{28}N_4O_8S_2Cl_2Ni$, **6**: C 43.48, H 3.93, N 7.80. Found: C 43.24, H 3.79, N 7.71. Selected IR frequencies (KBr disk, $cm^{-1}$): 3190(s, $\nu_{NH}$), 3084(w), 2975(w), 2935(w), 1609(s, def $\nu_{NH}$), 1571(w), 1461(s), 1435(s), 1287(m), 1116(vs), 1049(s), 996(w), 973(m), 959(m), 929(m), 888(w), 811(m), 767(s), 737(m), 721(w), 750(s), 652(w),


dx.doi.org/10.1021/ic300606g | Inorg. Chem. 2012, 51, 7625−7635

Table 1. Data Collection and Structure Refinement Parameters for Complexes 1, 3−7

| | 1 | 3 | 4 | 5·$CH_3CN$ | 6 | 7 |
|---|---|---|---|---|---|---|
| | $C_{26}H_{24}N_4O_8S_2Cl_2Ni$ | $C_{38}H_{30}N_4O_8S_2Cl_4Ni$ | $C_{26}H_{22}N_4O_8S_2Cl_2Br_2Ni$ | $C_{28}H_{25}N_5O_8S_2Br_2Cl_2Ni$ | $C_{26}H_{28}N_4O_8S_2Cl_2Ni$ | $C_{26}H_{22}N_4O_2S_2Ni$ |
| mol wt | 714.22 | 934.28 | 872.03 | 913.08 | 718.20 | 545.30 |
| cryst. system | orthorhombic | orthorhombic | triclinic | monoclinic | monoclinic | monoclinic |
| color | reddish yellow | reddish yellow | dark green | red | violet | dark brown |
| space group | $P2_12_12_1$ | $Pca2_1$ | $P\bar{1}$ | $P2_1/n$ | $P2_1/c$ | $P2_1/c$ |
| $a$ (Å) | 8.5779(6) | 21.635(5) | 8.618(5) | 12.2520(12) | 8.8510(15) | 11.7107(13) |
| $b$ (Å) | 10.2497(14) | 7.7408(17) | 10.792(5) | 19.3495(19) | 11.746(2) | 15.9712(17) |
| $c$ (Å) | 33.302(4) | 23.877(5) | 17.819(9) | 15.0922(15) | 16.841(3) | 13.3606(14) |
| $\alpha$ (deg) | 90.0 | 90.0 | 83.576(11) | 90.0 | 90.0 | 90.0 |
| $\beta$ (deg) | 90.0 | 90.0 | 75.352(18) | 107.613(2) | 120.627(7) | 110.296(3) |
| $\gamma$ (deg) | 90.0 | 90.0 | 73.700(8) | 90.0 | 90.0 | 90.0 |
| $V$ (Å$^3$) | 2928(5) | 3998.7(15) | 1537.5(14) | 3410.2(6) | 1506.6(5) | 2343.7(4) |
| $Z$ | 4 | 4 | 2 | 4 | 2 | 4 |
| $d_{calc}$(g cm$^{-3}$) | 1.620 | 1.552 | 1.884 | 1.778 | 1.583 | 1.547 |
| $\theta$ range (deg) | 2.08−26.14 | 1.71−18.85 | 2.25−32.08 | 1.76−27.88 | 2.23−25.24 | 1.85−19.39 |
| $\mu$ (mm$^{-1}$) | 1.044 | 0.914 | 3.596 | 3.247 | 1.015 | 7.051 |
| F(000) | 1464 | 1908 | 868 | 1824 | 740 | 2378 |
| refl./params. | 9089/427 | 14015/517 | 14721/445 | 42868/453 | 7831/196 | 12279 |
| unique refl. | 3619 | 2451 | 13203 | 7215 | 2365 | 1539 |
| $R_1$ [I > 2$\sigma$(I)][a] | 0.0887 | 0.0659 | 0.0458 | 0.0537 | 0.0381 | 0.0340 |
| $wR_2$ [I > 2$\sigma$][b] | 0.2172 | 0.1567 | 0.1266 | 0.1316 | 0.0941 | 0.0668 |
| GOF | 1.032 | 1.075 | 1.10 | 1.143 | 1.064 | 1.038 |
| res. dens. (eÅ$^{-3}$) | 1.036/−1.079 | 0.795/−0.412 | 1.790/−1.018 | 2.701/−1.811 | 0.787/−0.306 | 0.222/−0.239 |

[a] $R_1 = \sum||F_o| - |F_c||/\sum|F_o|$, [b] $wR_2 = \{\sum[w(F_o^2 - F_c^2)^2]/\sum w[(F_o^2)^2]\}^{1/2}$

638(w), 623(s), 590(w), 556(w), 491(m), 460(w), 424(m). EI mass spectrum $m/z$: 517.10 for $[(L2)_2Ni^{2+}-H^+]^+$, 231.09 $[(L2+H)]^+$. Absorption spectrum [$\lambda_{max}$, nm ($\varepsilon$, M$^{-1}$ cm$^{-1}$), in MeCN] 257 (16332), 302 sh (5116), 370 sh (575), 555 (13), 890 (14).

*[Ni(L3)$_2$], 7.* The ligand L3 (0.15 g, 0.615 mmol) was dissolved in 10 mL of dry DMF and to it was added solid NaH (0.017 g, 0.738 mmol), while a light yellow solution was generated. To the resulting solution was then added dropwise a DMF solution (5 mL) of $[Ni(H_2O)_6](ClO_4)_2$ (112 mg, 0.307 mmol). After complete addition, the solution color changed to light green that, on warming at ∼60 °C in a water bath for 30 min, changed to clear yellow solution. It was stirred for 2 h at room temperature. The solution was concentrated to half of its volume and was layered with ether and kept at 4 °C. After two days, dark brown needle shaped crystals obtained were filtered off and washed with ether and vacuum-dried (0.14 g, yield 85%). Elemental analysis calcd for $C_{26}H_{22}N_4O_2S_2Ni$, 7: C 57.27, H 4.07, N 10.27. Found: C 57.20, H 3.99, N 10.22. Selected IR frequencies (KBr disk, cm$^{-1}$): 3057(w), 3001(w), 2931(w), 1611(vs, $\nu_{CO}$), 1589(vs), 1574(vs), 1561(vs), 1465(vs), 1432(s), 1354(vs), 1289(s), 1265(m), 1089(w), 1045(m), 1023(w), 926(s), 822(m), 757(s), 695(m), 644(m), 513(m), 476(m), 458(w), 436(w), 406(w). EI mass spectrum $m/z$ (%): 545.12 $(M+H)^+$, 100) for $[\{(L3)_2Ni\} + H]^+$, 245.10 $(L3+H)^+$, 30). Absorption spectrum [$\lambda_{max}$, nm ($\varepsilon$, M$^{-1}$ cm$^{-1}$), in $CH_2Cl_2$] 319 (9715), 346 (10964), 380 sh (5220), 560 (27), 665 sh (14), 851 (70).

*Physical Measurements.* The Fourier transform infrared spectra of the ligand and the complexes were recorded on a Thermo Nicolet iS10 spectrometer using KBr pellets in the range 4000−400 cm$^{-1}$. The electronic spectra were recorded on an Agilent 8453 diode array spectrophotometer. Elemental analyses were carried out on a Perkin-Elmer 2400 series-II CHNS analyzer. Electron paramagnetic resonance (EPR) spectra of the electrochemically generated Ni$^{III}$ and Ni(I) species were obtained in $CH_3CN$ using a Bruker-EMX-1444 EPR spectrometer at 77 K. Mass spectra were recorded on Micromass Q-Tof micro. Solution conductivity was measured using a CHEMILINE conductivity meter, CL220, $^1$H NMR spectra were recorded on Bruker DPX-300. Redox potentials were measured using CHI 1120A potentiometer. For constant potential electrolysis experiment platinum mesh working electrode was used and solute concentration was kept of ∼1 × 10$^{-3}$ or ∼3 × 10$^{-4}$ molar.

*X-ray Diffraction Studies.* Crystals of **1**, **3**, **4**, and **5** were grown by diffusion of dry diethyl ether into the concentrated $CH_3CN$ solution of the respective complexes at low temperatures (−10 °C for **1** and 4 °C for **3**−**5**). Violet block-shaped crystals of **6** and the deep brown crystals of **7** were obtained by layering ether on top of the $CH_3CN$ or DMF solution of **6** and **7**, respectively, at 4 °C. Single-crystal intensity measurements for **1** were collected at room temperature, while those for **3**, **6**, and **7** were collected at 120 K and for **4** and **5** at 90 K with a Bruker Smart APEX II CCD area detector using Mo K$\alpha$ radiation ($\lambda$ = 0.71073 Å) with a graphite monochromator. The cell refinement, indexing, and scaling of the data set were carried out using Apex2 program.[13] All structures were solved by direct methods with SHELXS, and refined by full-matrix least-squares based on $F^2$ with SHELXL[14] whereas the other calculations were performed using WinGX, Version 1.80.05.[15] The crystal of **4** was a pseudomerohedral twin. One of the two perchlorate anions in **1**, **4**, and **5** was found to be disordered over two orientations. No such disorder of perchlorate anions has been encountered for complex **3** and **6**. The positions of the C-bound H atoms were calculated assuming ideal geometry and refined using a riding model. Figures showing displacement parameters were created with ORTEP3.[16] Crystal data for the complexes **1** and **3**−**7** are summarized in Table 1. Additional crystallographic data and refinement details are available in the Supporting Information.

## RESULTS AND DISCUSSION

**Synthesis and Characterization.** Condensation of pyridine-2-carboxaldehyde or of its substituted forms with an equimolar amount of 2-(methylthioaniline) in $CH_3OH$ or toluene produced the ligands $^X$L1 (Scheme 1) in high yield. All the Schiff bases display an intense stretch in the range 1620−1630 cm$^{-1}$ and a medium intense stretch within the range 666−696 cm$^{-1}$ in their IR spectra[17] that correspond to the $\nu_{C=N}$ (of imine) and $\nu_{C-S}$ (of thioether),respectively. Yellow thick oil of L2 was obtained from the $NaBH_4$ reduction of L1 in $CH_3OH$ after usual workup. Presence of an intense peak at 3358 cm$^{-1}$


dx.doi.org/10.1021/ic300606g | Inorg. Chem. 2012, 51, 7625−7635

corresponding to $\nu_{N-H}$ is observed in the IR spectrum of L2. The amide ligand L3 has been synthesized from the condensation reaction of pyridine-2-carboxylic acid with 2-(methylthioaniline) in pyridine at elevated temperature in presence of triphenylphosphite. The presence of $\nu_{N-H}$ at 3278 $cm^{-1}$ and $\nu_{CO}$ at 1682 $cm^{-1}$ in the IR spectrum of L3 confirms the amide functional group. To ensure the ligation of two ligands to the $Ni^{II}$ salt, $[Ni(H_2O)_6](ClO_4)_2$ was chosen as a starting material. Dilute solutions of $[Ni(H_2O)_6](ClO_4)_2$ were added dropwise to the ligand solutions (metal to ligand ratio 1:2) to yield the desired bis complexes.

The red-shifted $\nu_{C=N}$ and $\nu_{C-S}$ of the corresponding ligands in complexes **1**–**5**, found in the ranges 1583–1596 $cm^{-1}$ and 636–647 $cm^{-1}$, respectively, indicate imine N and thioether S coordination to $Ni^{II}$ . Complex **5**, in addition exhibits a weak stretch at 2251 $cm^{-1}$, corresponds to $\nu_{C\equiv N}$ of a $CH_3CN$ molecule present as a solvent of crystallization. The red-shifted $\nu_{N-H}$ at 3190 $cm^{-1}$ (for free L2 3358 $cm^{-1}$) observed in the IR spectrum of **6** indicates the amine N coordination. The IR spectra of **1**–**6** feature an intense broad band at ~1100 $cm^{-1}$ that indicates the presence of perchlorate as counteranion. Deprotonation of the amide proton of L3 using a strong base like NaH in DMF and reaction with $[Ni(H_2O)_6](ClO_4)_2$ produced **7**, the IR spectrum of which displays an intense and red-shifted ($\nu_{CO}$ = 1682 $cm^{-1}$ for L3) stretch at 1611 $cm^{-1}$, corresponding to $\nu_{CO}$. Conductivity measurement of **7** in DMF ($\Lambda$ = ~8 $\Omega$ $Mol^{-1}$ $cm^{-1}$) reveals its electroneutrality. The absence of $\nu_{N-H}$ and the presence of red-shifted $\nu_{CO}$ strongly support the amidato $N^-$ coordination to $Ni^{II}$. Solution conductivity of **1**–**6** in $CH_3CN$ corroborates their 1:2 electrolytic behavior ($\Lambda$ ranges from 220 to 245 $\Omega$ $Mol^{-1}$ $cm^{-1}$).[18] Mass spectral results and microanalytical data, in addition to the information of **1**–**7**, further support their formulations as stated.

*Structures of the Complexes: $[Ni(^XL1)_2](ClO_4)_2$ (**1** and **3**–**5**).* A perspective view of the cationic part of a representative complex, $[Ni(L1)_2](ClO_4)_2$, **1**, with its atom labeling scheme is shown in Figure 1, and figures for the other complexes, **3**–**5**, are given in the Supporting Information (Figures S1–S3). Selected average bond distances and angles are listed in Table 2. Distorted octahedral coordination geometry for Ni is observed in all cases. Two tridentate ligands $^XL1$ (Scheme 1) each consisting of a pyridine N, an imine N and a thioether S donor atom are arranged in a meridional fashion to $Ni^{II}$. The $Ni-N_{py}$, $Ni-N_{imine}$, and Ni–S distances vary according to the average $Ni-N_{py}$, $Ni-N_{imine}$, and Ni–S[19,20] distances tabulated in Table 2.

**Table 2. Selected Average Bond Distances (Å) of $[Ni(^XL1)_2](ClO_4)_2$ Complexes 1, 3, 4, 5**

| | 1 | 3 | 4 | 5 |
|---|---|---|---|---|
| | X = 6-H | X = 6-*p*-ClPh | X = 6-Br | X = 5-Br |
| Ni–N(py) | 2.083(7) | 2.110(12) | 2.136(6) | 2.086(3) |
| Ni–Ni(im) | 2.036(6) | 2.025(13) | 2.041(3) | 2.030(3) |
| Ni–S(thioether) | 2.439(2) | 2.475(4) | 2.4229(13) | 2.4383(11) |

Scrutiny of the structural data reveal that the average $Ni-N_{py}$ distances follow the trend **1**~**5** < **3** < **4** as a consequence a weaker $N_{py}$ donor strength of the respective $^XL1$ ligand.

*$[Ni(L2)_2](ClO_4)_2$, **6**.* An ORTEP diagram of the cationic part of **6** with the atom labeling scheme is illustrated in Figure 2.

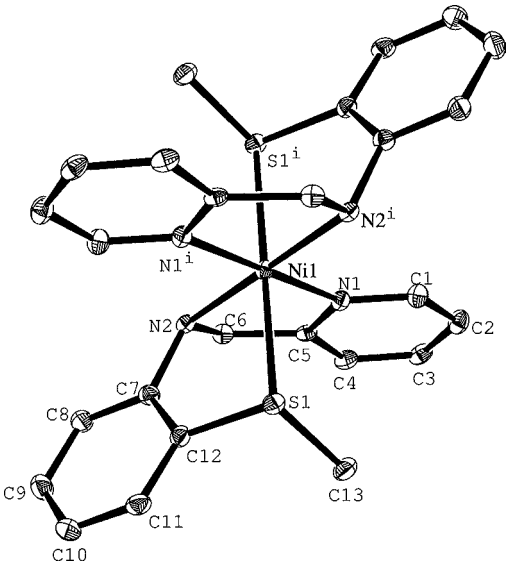


**Figure 2.** Thermal ellipsoid (probability level 50%) plot of $[Ni(L2)_2]^{2+}$ (cation **6**) with the atom labeling scheme. H atoms are omitted for the sake of clarity.

The structure has crystallographic inversion symmetry. The secondary amine N apparently gives the ligand greater flexibility than the imine N and allows for facial coordination of the two L2 ligands. The Ni–N(am) distance is 2.082(2) Å, 0.046 Å longer than the average Ni–N(im) distance of **1** and is comparable to the Ni–N(am) distances of other reported $Ni^{II}$ complexes of amino-pyridine ligands.[11a–e] The Ni–N(py) distance is 2.070(2) Å, and the Ni–S(thioether) distance is 2.4422(7) Å. The amine proton is hydrogen bonded to one of the perchlorate oxygen atoms with the N2···O4 distance of 2.896(3) Å and N2–H2A···O4 angle of 177.0°.

*$[Ni(L3)_2]$, **7**.* A perspective view of **7** with labeled atoms is shown in Figure 3. Two L3 ligands are meridionally coordinated via their pyridine N, amidato N, and thioether S donors. The average $Ni-N_{py}$, $Ni-N_{amide}$, and Ni–S distances are 2.059(4) Å, 2.016(4) Å, and 2.4442(15) Å, respectively,

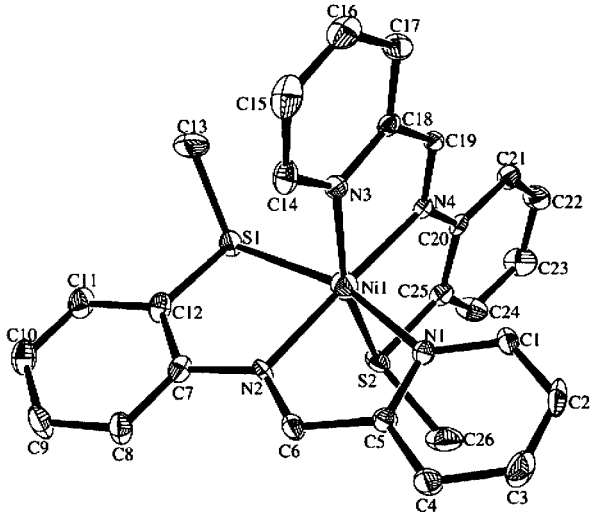


**Figure 1.** Thermal ellipsoid (probability level 50%) plot of $[Ni(L1)_2]^{2+}$ (cation **1**) with the atom labeling scheme. H atoms are omitted for the sake of clarity.


dx.doi.org/10.1021/ic300606g | Inorg. Chem. 2012, 51, 7625–7635

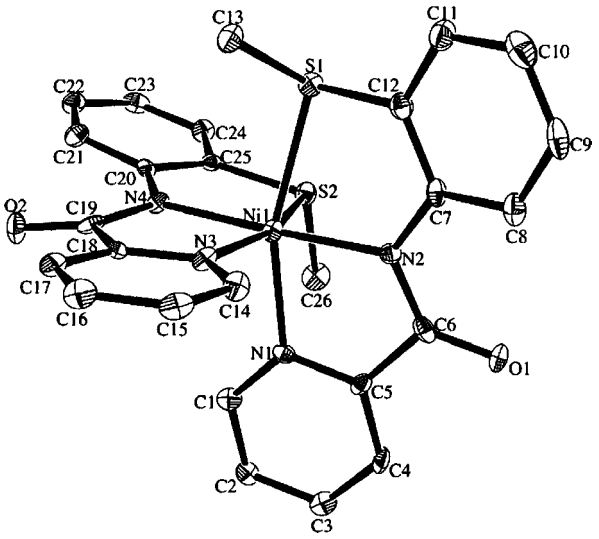


**Figure 3.** Thermal ellipsoid (probability level 50%) plot of $[(L3)_2Ni]$, **7**, with the atom labeling scheme. H atoms are omitted for clarity.

comparable to those of reported $N_4S_2Ni^{II}$ complexes of ligands having similar types of donor atoms.[4a,k] The average Ni−N(amide) distance is 0.02 Å and 0.066 Å shorter than the average Ni−N(im) and Ni−N(am) distances found in **1** and **6** and indicates stronger donation of amidato $N^-$ than either the imine or amine N donor. The N2−C6 and C6−O1 distances of 1.351(7) Å and 1.236(6) Å, respectively, support the delocalization of the negative charge on deprotonated amidato N atom over the three atoms (N2, C6, and O1) of the amide functional group. Similar observations have previously been reported.[4b]

**Electronic Spectra.** The electronic spectra taken in $CH_3CN$ of complexes **1**, **6**, and **7** are shown in Figure 4, and

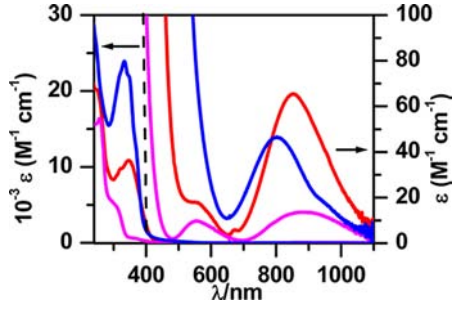


**Figure 4.** Electronic absorption spectra of $[Ni(L1)_2](ClO_4)_2$, **1** (blue), $[Ni(L2)_2](ClO_4)_2$, **6** (pink), and $[Ni(L3)_2]$, **7** (orange) in $CH_3CN$.

the spectral data of **1**−**7** are tabulated in Table 3. The spectra of **1**−**5** exhibit similar patterns in the 200−1100 nm region (see Supporting Information, Figure S4). In the visible range, compounds **1**−**5** display a broad and weak lower energy band in the range 800−900 nm (for **1**−**5** this band are at 803, 870, 880, 890, and 805 nm respectively), attributable to $^3A_{2\ g}(F)\rightarrow{}^3T_{2\ g}(F)$ transition in case of an octahedral $Ni^{II}$ parentage.[21] Descending into a lower symmetry causes splitting of both $^3T_{2g}(F)$ and $^3T_{1g}(F)$ terms due to spin−orbit coupling; therefore, the lowest energy band, $\nu_1$, can be treated as an envelope of several overlapped transitions, hence broad in nature.[22] The $\nu_1$ value linearly decreases for complexes **1**→**4** ($\nu_1$ = 12453 $cm^{-1}$, 11494 $cm^{-1}$, 11363 $cm^{-1}$, and 11235 $cm^{-1}$ for **1**−**4**, respectively), and indicates weakening of the ligand field strength, which is strongly supported from an increasing trend of the average Ni−$N_{py}$ distances (see Table 2). As the average Ni−$N_{py}$ distances in **1** and **5** are virtually identical a very close $\nu_1$ value for these two compounds is expected and observed (for **5**, $\nu_{1=}$ 12422 $cm^{-1}$). Ligand $^{6,Me}$L1 with an electron donating -Me substituent, *ortho* to the pyridine N is expected to have better $N_{py}$ donor strength than the unsubstituted L1 and in consequence a higher $\nu_1$ value for **2** than **1**. However, for **2**, a 459 $cm^{-1}$ lower value of $\nu_1$ than **1** is observed suggests not only the electronic but also a steric factor is operating for such lowering of $\nu_1$ value. This lowering of $\nu_1$ will be more prominent for a bulky −I substituent (−Br in **4**) than a +I substituent (−Me in **2**) one, attached *ortho* to $N_{py}$. Other higher energy transitions (see Table 4) are due to the intra-ligand $n\rightarrow\pi^*$ and $\pi\rightarrow\pi^*$ charge transfer transitions.[12,23]

**Table 3. Electronic Spectral Data of $Ni^{II}$ Complexes, in $CH_3CN$ at 298 K**

| compd | $\lambda_{max}$, nm ($\varepsilon$ $M^{-1}$ $cm^{-1}$) |
|---|---|
| **1** | 234 sh (30290), 246 sh (26160), 318 sh (22170), 333 (23790), 347 sh (21910), 366 sh (13650), 520 sh (166), 803 (46), 940 sh (22) |
| **2** | 237 sh (25700), 248 sh (23760), 320 sh (21700), 339 (25140), 354 sh (23420), 372 sh (14130), 870 (40) |
| **3** | 205 sh (66070), 243 (44565), 270 sh (33730), 347 (18400), 382 sh (10530), 880 (42) |
| **4** | 248 (29125), 264 sh (25550), 293 (18470), 333 (15560), 351 (15910), 370 sh (12700), 890 (30) |
| **5** | 270 (21770), 330 sh (21460), 342 (23520), 357 (22770), 380 sh (14200), 805 (45) |
| **6** | 257 (16332), 302 sh (5116), 370 sh (575), 555 (13), 890 (14) |
| **7** | 320 (10244), 341 (11060), 560 sh (27), 665 sh (14), 851 (65) [319 (9715), 346 (10964), 560 sh (30), 665 sh (14), 851 (70)][a] |
| **L1** | 253 (17650), 266 sh (17200), 365 (3870)[a] |

[a]Measured in $CH_2Cl_2$

The spectra of **6** and **7** feature two distinct, well separated (more than 250 nm), weak lower energy bands [$\lambda_{max}$ ($\varepsilon$ in $M^{-1}$ $cm^{-1}$) for **6**, 890 nm (57) and 555 nm (46); for **7**, 851 nm (69) and 560 nm (27)] correspond to $\nu_1$ and $\nu_2$ transitions, respectively. As these bands are well separated, a little mixing of these two transitions are expected that will provide a more accurate value of the Racah parameter B[24] and the nephelauxetic ratio $\beta$,[25] which measures the degree of covalency for a particular complex. The $\beta$ values for **6** and **7** are 0.84 and 0.64, respectively. The lower $\beta$ value in **7** is due to the planarity and conjugation of the pyridine and phenyl rings of the L3 ligand, unlike ligand L2 in **6**.

**Redox Properties.** To investigate the susceptibility toward oxidation or reduction of the nickel(II) center in complexes **1**−**7**, the cyclic voltammograms (CV) were recorded for all the complexes in $CH_3CN$ using same cell set up. A three electrode cell set-up such as platinum, saturated calomel electrode (SCE), and a platinum wire as a working, reference, and auxiliary electrodes, respectively, has been used for measurement of the potentials. Results are summarized in Table 4. Each of the complexes **1**−**5** shows two quasi-reversible one electron reduction waves correspond to $Ni^{II}\rightarrow Ni^{I}$ and subsequent $Ni^{I}\rightarrow Ni^{0}$ transformation (Supporting Information, Figure S5). Schiff base ligands, $^{X}$L1, have pyridine, imine N, and thioether S donor sites, all of which has a $\pi$-acceptance property; therefore, they are expected to stabilize the lower oxidation states of nickel, such as $Ni^{I}$ and $Ni^{0}$ states.


dx.doi.org/10.1021/ic300606g | Inorg. Chem. 2012, 51, 7625−7635

Table 4. Electrochemical Data[a] for the Complexes 1−7 and Other Selected $NiN_4S_2$ Complexes

| | $E_{1/2}$, V ($\Delta E_p$,[b] mV) | | | |
|---|---|---|---|---|
| | $Ni^I/Ni^0$ | $Ni^{II}/Ni^I$ or $Ni^{II}/Ni^0$[c] | $Ni^{II}/Ni^{III}$ | ref |
| **1** | −0.84 (131) | −0.65 (74) | | this work |
| **2** | −0.88 (90) | −0.60 (91) | | this work |
| **3** | −0.79 (72) | −0.54(85) | | this work |
| **4** | −0.78 (91) | −0.45 (104) | | this work |
| **5** | −0.77 (102) | −0.57 (97) | | this work |
| **6** | | −1.28[c] | | this work |
| **7** | | | +0.84 (60) | this work |
| $[Ni^{III}(Ph_2L)]PF_6$ | | | +0.45 (80) | 5c |
| $[Ni^{III}(Ph_3L)]PF_6$ | | | +0.46(90) | 5c |
| $[Ni^{III}(Np_2L)]PF_6$ | | | +0.43 (80) | 5c |
| $[Ni^{III}(Np_3L)]PF_6$ | | | +0.45 (80) | 5c |
| $[Ni^{II}(Atep)_2](ClO4)_2$ | | −1.35[d] | | 11b |
| $[Ni^{II}(L4)_2](ClO4)_2$ | | −1.23 (140)[e] | | 11d |
| $[Ni^{II}(dtdida)_2](ClO4)_2$ | | | +1.17 (70) | 11j |
| $[Ni^{II}(bpzctb)]$ | | | +1.04 (120) | 4a |
| $[Ni^{II}(bpctb)]$ | | | +0.84 (200) | 4k, a |
| $[Ni^{II}(SEtaaiNEt)_2]^{2+}$ | | | +0.80 (90) | 11k |

[a]Potentials are vs SCE ($F_c/F_c^+$ couple in $CH_3CN$, $E_{1/2}$ = 0.43 V), scan rate 50 mV/s, supporting electrolyte, *n*-$Bu_4NClO_4$ (0.1 M). [b]$\Delta E_p = E_{pa} - E_{pc}$. [c]$E_{pc}$ of $Ni^{II}/Ni^0$. [d]$E_{pc}$ of $Ni^{II}/Ni^0$ vs $Ag^+$. [e]Potential is vs $F_c/F_c^+$.

The negative potentials of **1** are more anodic than the potential needed to reduce the ligand L1 ($E_{pc}$ = −1.72 V see Supporting Information, Figure S6) in $CH_3CN$. X-ray structural (longer Ni−$N_{py}$ distance) and electronic spectral (red-shifted $\nu_1$ value) data of the complexes **1**−**5** revealed a decreasing trend of $N_{py}$ donor strength such as **1**∼**5** > **2** > **3** > **4** (*vide supra*), in consequence, an easy $Ni^{II}\rightarrow Ni^I$ reduction; that is, a more anodic $E_{1/2}$ value for $Ni^{II}/Ni^I$ couple is expected and observed, shown in Figure 5. A 200 mV anodic shift of the $E_{1/2}$ value for $Ni^{II}/Ni^I$ couple is evident, going from **1** ($E_{1/2}$ = −0.65 V vs SCE) to **4** ($E_{1/2}$ = −0.45 V vs SCE). To the best of our knowledge, other reported $Ni^{II}N_4S_2$ complexes display either an irreversible reduction or their reduction is not reported or the reduction is of ligand centered in origin.[11k] Low $Ni^{II}\rightarrow Ni^I$ reduction potential is reported for $Ni^{II}$ complexes with flexible ligand(s) containing soft donors, so they can adopt the required geometry needed to stabilize the $Ni^I$ and $Ni^0$ states.[6a] Quite in contrast, in the present study, the donor sites of $^X$L1 are coplanar, restrained to occupy the fixed geometric sites and not flexible enough to adopt Td geometry, required for stabilizing $Ni^0$. To the best of our knowledge, with planar ligand system these complexes comprise the first example of a series of $NiN_4S_2$ complexes where quasi-reversible redox responses correspond to $Ni^{II}\rightarrow Ni^I$ and $Ni^I\rightarrow Ni^0$ transformations are evident.

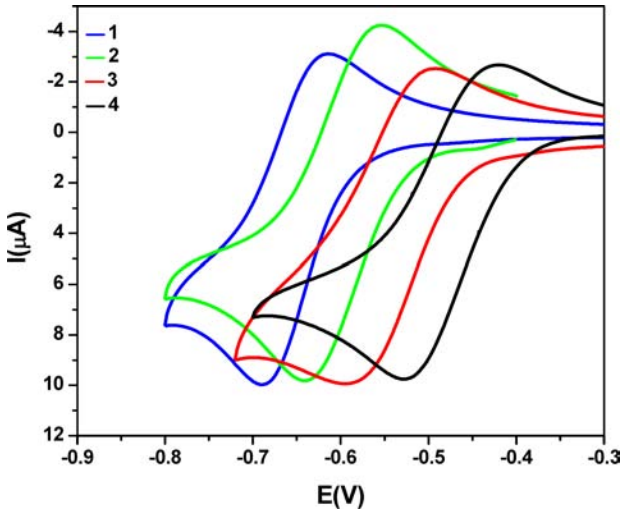


**Figure 5.** Cyclic voltammograms of **1** (blue), **2** (green), **3** (red), and **4** (black) in $CH_3CN$ containing 0.1 M N(*n*-Bu)$_4ClO_4$ as a supporting electrolyte at 298 K at a platinum working electrode at a scan rate 50 mV $s^{-1}$ using SCE as reference electrode.

To clarify whether the first reduction is of metal or ligand centered that will generate either a $Ni^I$ species or a $Ni^{II}$-($L1^{\bullet-}$) species respectively, the controlled potential electrolysis at an applied potential of −0.79 V and the EPR spectral measurement of the electro-generated species in $CH_3CN$ at 77 K were performed for a representative complex **1**, associated with a low $\Delta E_p$ value (more toward reversible) of 74 mV. The EPR spectrum of the electrochemically generated species displays a rhombic anisotropic signal with three principal *g* values at 2.059, 2.010, and 1.915 (shown in Figure 6); those are far from 2.002 expected for a ligand radical anion indicating that the unpaired electron primarily resides in the d orbital of the $Ni^I$


**Figure 6.** X-band EPR spectrum of electrochemically generated $Ni^I$ species (from electrolysis of a $CH_3CN$ solution of **1**) at 77 K (conditions: frequency, 9.475 GHz; modulation, 5G; power, 0.189 mW).


dx.doi.org/10.1021/ic300606g | Inorg. Chem. 2012, 51, 7625−7635

ion, not on the ligand frame. Furthermore, a five line splitting of the $g$ = 2.01 peak is due to the super hyperfine coupling (coupling constant $A_{\|}^{N}$ of 10 × $10^{-4}$ $cm^{-1}$) of the unpaired electron spin on $Ni^{I}$ to the nuclear spin of two nitrogen atoms, possibly of the two trans imine N of L1.[3d] The electronic spectrum of the electrolyzed solution features a lower energy band at ~970 nm (shown in Figure 7), red-shifted than that of

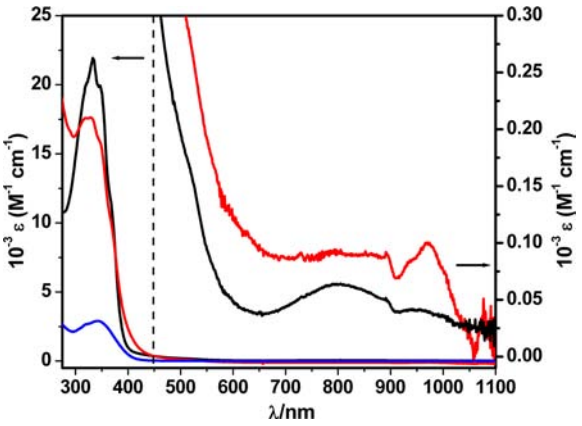


**Figure 7.** Electronic absorption spectra of 1 (black) and of the coulometrically reduced species, $[(L1)_2Ni^{I}]^{+}$ (red) and ligand decoordinated $Ni^{0}$ species (blue) containing 0.1 M $N(n\text{-}Bu)_4ClO_4$ at 298 K in $CH_3CN$.

the parent complex **1**. Other higher energy transitions [$\lambda_{max,}$ nm ($\varepsilon$, $M^{-1}$ $cm^{-1}$) for $Ni^{I}$ species: 309 sh (17020), 330 (17560), 348 sh (15700), 366 sh (10530), 970 (100)] are similar to those of **1**. However, this electrochemically generated $Ni^{I}$ species is not stable enough, highly sensitive to dioxygen and revert back with time to $Ni^{II}$ along with partial complex decomposition products, most possibly, due to the disproportionation of $2Ni^{I}$ →$Ni^{II}$ + [$Ni^{0}$ + L1] (*vide infra*). We have attempted to investigate the behavior of the electrochemically reduced species correspond to the second reduction wave of $E_{1/2}$ = −0.84 V. The original reddish brown solution of **1** changes to pale yellow upon electro-reduction at −1.2 V, the electronic spectrum of which is identical to that of the ligand (Figure 7). Therefore, the equation of electron transfer reaction is as $Ni^{II}$ + $2e^{-}$ → $Ni^{0}$ + $^{X}$L1. Because $^{X}$L1 is planar, it can not provide the preferred *Td* geometry for $Ni^{0}$ state, hence detached from metal.

The CV scans of **6** in $CH_3CN$ have been displayed in Figure 8 and the plausible transformations followed by electron transfer reactions have been shown in Scheme 2. The first scan (blue trace) was started from the resting potential of −0.4 V toward anodic that does not show any response up to +0.6 V. The reverse scan from +0.6 V → −1.6 V features a strong reductive response at $E_{pc}$ = −1.28 V (close to the $E_{1/2}$ value of $Ni^{I}$→$Ni^{0}$ reduction of complexes **1**−**5**) correspond to the $Ni^{II}$→$Ni^{0}$ reduction (Scheme 2: A→B transformation). A broad, anodic stripping potential at $E_{pa}$ = +0.11 V with a shoulder at +0.25 V is observed as a result of the $Ni^{0}$→$Ni^{II}$ reoxidation process (blue trace in Figure 8), which was absent when the fresh solution was scanned from −0.4 V→+0.6 V.

This response has only been seen when the cathodic scan up to a high negative potential of −1.6 V is performed that generates $Ni^{0}$ species which will get reoxidized back. Large $\Delta E_p$ value firmly indicates that this process is irreversible and a remarkable structural reorganization takes place during $Ni^{II}$→

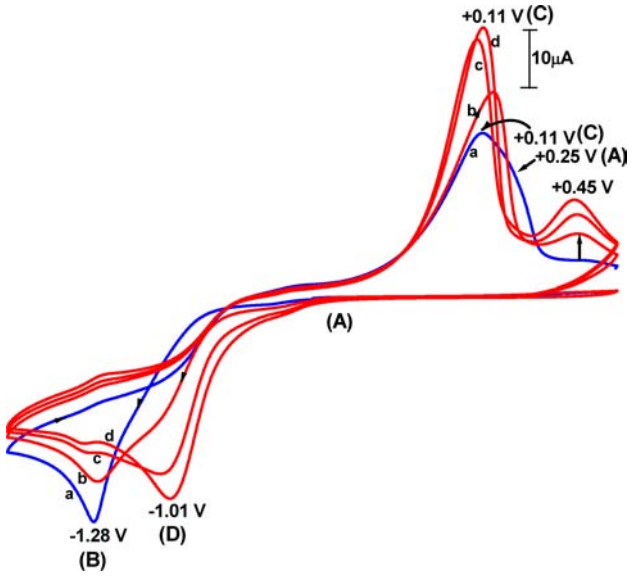


**Figure 8.** Cyclic voltammograms (a→d, repetitive scans) of **6** in $CH_3CN$ containing 0.1 M $N(n\text{-}Bu)_4ClO_4$ as supporting electrolyte at 298 K at a platinum working electrode at a scan rate 50 mV $s^{-1}$ using SCE as reference electrode, showing first scan (a: blue trace) and transformation to $[(L2)_2Ni(CH_3CN)_2](ClO_4)_2$ (b, c, d: red traces).

$Ni^{0}$ reduction. Flexibility of L2 coordination in **6** is capable of stabilizing $Ni^{0}$ state as shown in Scheme 2. During reoxidation of $Ni^{0}$→$Ni^{II}$ the solvent molecules ($CH_3CN$) and dangling pyridine N donors (−NH−$CH_2$-py) of L2 compete to occupy two empty sites to fulfill hexa-coordination, preferred for $Ni^{II}$ state (B→A + C in Scheme 2). Most possibly due to this reason, a broad anodic reoxidation response (with $ip_a \ll ip_c$; or $ip_c = ip_a$ of +0.11 V peak + $ip_a$ of +0.25 V peak, see blue trace in Figure 8) at $E_{pa}$ = +0.11 V with a shoulder at +0.25 V is observed, owing to the formation of two $Ni^{II}$ species, A and C, shown in Scheme 2. Successive scans between +0.6 V → −1.6 V anodically shifted the $E_{pc}$ of $Ni^{II}$ →$Ni^{0}$ transformation from −1.28 to −1.01 V (Figure 8). The $E_{pc}$ of −1.01 V is responsible for C→D transformation. The solvated species C is expected to reduce more easily than A where L2 is fully coordinated. Similar CV scan profile for a $Ni^{II}$ complex, $[Ni(Atep)_2](ClO_4)_2$ (where Atep = [(2′-aminophenylthio)ethyl)pyridine]) in $CH_3CN$ is reported.[11b] The newly developed response at +0.45 V, possibly is due to the reoxidation of a more solvated $Ni^{II}$ species than D, generated during the time of repetitive reduction−oxidation processes.

The CV of **7** in $CH_3CN$ displays a reversible oxidative response at $E_{1/2}$ = +0.84 V vs SCE ($E_{pa}$ = +0.87 V, $E_{pc}$ = +0.81 V and $\Delta E_p$ = 60 mV) that has been shown in Figure 9. No other redox response within the potential window of −1.6 V to +1.6 V has been observed. The peak current function, $i_p/\nu^{1/2}$ is independent of the scan rates shown in the inset of Figure 9. The value of $i_{pa}/i_{pc} \approx 1$ clearly indicates the reversibility of the $Ni^{II}/Ni^{III}$ couple. At least two other $Ni^{II}N_4S_2$ complexes, namely $[Ni^{II}(bpctb)]^{4k}$ and $[Ni^{II}(bpzctb)]^{4a}$ (where $H_2$bpctb =1,4-bis[*o*-(pyridine-2-carboxamidophenyl)]-1,4-dithiobutane and $H_2$bpzctb =1,4-bis[*o*-(pyrazine-2-carboxamidophenyl)]-1,4-dithiobutane; H are dissociable amide protons) are reported where a closely similar donor environment surrounding $Ni^{II}$ ion, as in **7**, are there. $[Ni^{II}(bpctb)]$ exhibits a quasireversible oxidation virtually at the same potential but with a much larger $\Delta E_p$ value (200 mV) than **7** (see Table 4). Therefore,


dx.doi.org/10.1021/ic300606g | *Inorg. Chem.* 2012, 51, 7625−7635

**Scheme 2. Structures of the Complexes Involved in the Most Plausible Pathway of Repetitive Electron Transfer Reaction of 6 in MeCN**

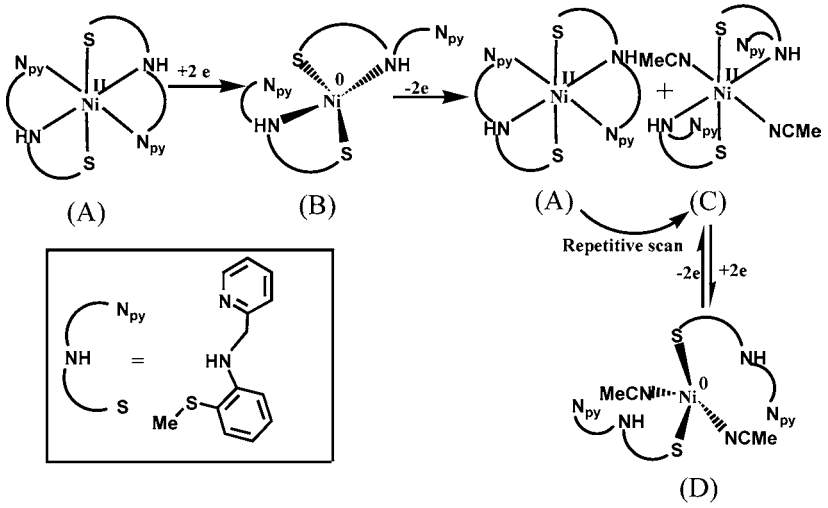


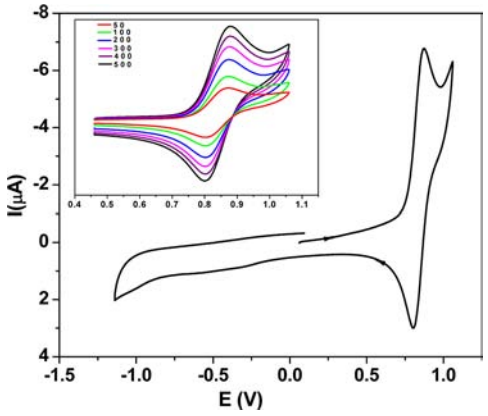


**Figure 9.** Cyclic voltammograms (scan rate 50 mV/s) of 7 in $CH_3CN$ containing 0.1 M $N(n\text{-}Bu)_4ClO_4$ as supporting electrolyte at 298 K at a platinum working electrode at a scan rate 50 mV $s^{-1}$ using SCE as reference electrode.

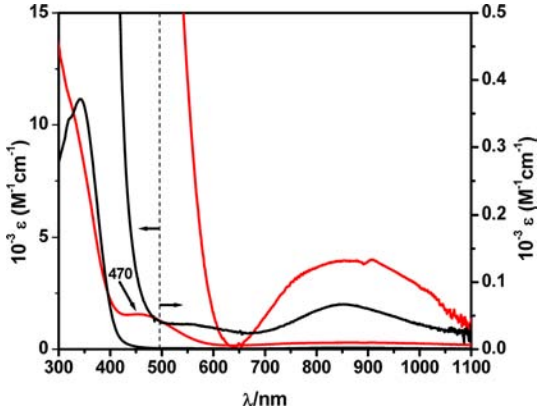


**Figure 10.** Electronic absorption spectra of 7 (black) and of the coulometrically generated oxidized species $[(L3)_2Ni^{III}]^+$ (red) containing 0.1 M $N(n\text{-}Bu)_4ClO_4$ at 298 K. The arrow indicates the Y-scale of the peaks from dashed line.

Mukherjee and co-workers have revisited the stability of the electrochemically generated $Ni^{III}$ species, $[Ni^{III}(bpctb)]^+$ and compared its stability and other electronic properties (UV−vis, EPR) to their electro-oxidized $Ni^{III}$ species, $[Ni^{III}(bpzctb)]^+$ derived from the $Ni^{II}$ precursor $[Ni^{II}(bpzctb)]$ where a lower $\Delta E_p$ value of 120 mV is evident for the $Ni^{II}/Ni^{III}$ redox couple.[4a] A much lower $\Delta E_p$ value of 60 mV for the $Ni^{II}/Ni^{III}$ couple of 7, therefore, tempted us to investigate the stability and electronic properties of the electrochemically oxidized species $[(L3)_2Ni]^+$ in $CH_3CN$. Constant potential electrolysis at an applied potential of +1.2 V generates a dark brown color that is stable at 298 K for 2−3 days. The electronic spectrum of electrochemically generated species, $[(L3)_2Ni^{III}]^+$ (Figure 10) features a new band at 470 nm [$\lambda_{max}$, nm ($\varepsilon$, $M^{-1}$ $cm^{-1}$) for $Ni^{III}$ species: 335 sh (9990), 470 (1560), 860 (130); see Supporting Information Figure S7 for UV−vis traces taken during the course of coulometric oxidation], as reported.[4a] The EPR spectrum of $[(L3)_2Ni^{III}]^+$ displays an anisotropic rhombic signal with three principal $g$ values at 2.140, 2.097, and 2.044, which are far from $g$ = 2.002, supporting strongly the metal centered oxidation and hence its formulation as $[(L3)_2Ni^{III}]^+$ and not as $[(L3^{\bullet+})(L3)Ni^{II}]^+$. The trend of $g$ values such as $g_\perp < g_\parallel$ indicates a $d_{x^2-y^2}$ ground state of $Ni^{III}$ ion. Furthermore, a poorly resolved super-hyper-fine, nine-line splitting of the $g$ = 2.04 component, shown in Figure 11, firmly supports the coupling of the unpaired nickel $e_g$ electron spin to the nuclear spin of four coordinated N ($2nI$ +1 = 9 lines, where $I$ =1) donor atoms of two L3 ligands. The $A_\parallel^N$ value of ~12 × $10^{-4}$ $cm^{-1}$ found for this super-hyper-fine splitting is similar to the $A_\parallel^N$ value reported before for Ni(I) complexes of general formulas $[Ni(terpy)(SR)_2(CO)]^-$ (where terpy = terpyridine, R= 2,4,6-($i$-$pr$)$_3C_6H_2$ or $C_6F_5$),[3d] however, a bit less than the value reported for $Ni^{III}N_4S_2$ complexes, which is ~28 × $10^{-4}$ $cm^{-1}$.[5c]

## CONCLUSIONS

A series of seven bis-$Ni^{II}$ pseudo-octahedral complexes based on the use of $N_2S$ donor tridentate ligands have been synthesized. These include five pyridine-substituted imines, one amine, and one amido central N atom variants. To the best of our knowledge, complexes **1**−**5** are the first examples of a series of $Ni^{II}N_4S_2$ complexes that display quasi-reversible responses for $Ni^{II}$→ $Ni^{I}$ reduction. Electrochemically generated $[Ni^{I}(L1)_2]^+$ species display a rhombic EPR signal (g values at 2.059, 2.011, and 1.998). Imine and pyridine N and thioether S donors are thus seen to stabilize the $Ni^{I}$ state. In the present


dx.doi.org/10.1021/ic300606g | Inorg. Chem. 2012, 51, 7625−7635

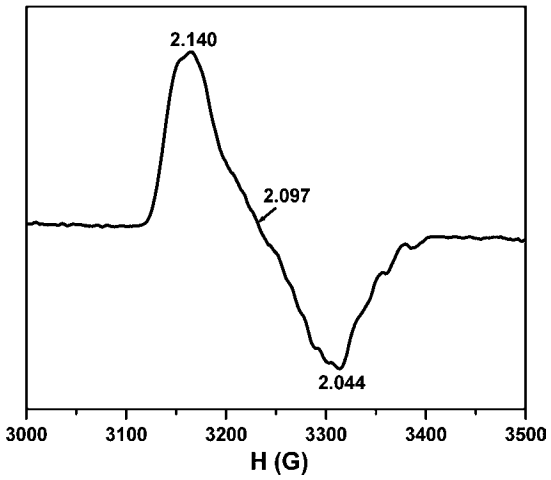


**Figure 11.** X-band EPR spectrum of electrochemically generated $Ni^{III}$ species (from electrolysis of a $CH_3CN$ solution of **7**) at 77 K (conditions: frequency, 9.475 GHz; modulation, 5G; power, 0.189 mW).

study we have outlined a correlation between donor strength of the $N_2S$ donor set and the accessibility of different oxidation states of Ni.

## ■ ASSOCIATED CONTENT

### Ⓢ Supporting Information

ORTEP of **3**, **4**, and **5**, cyclic voltammograms of **1**−**5** showing both reduction waves, electronic spectra of **1**−**5** taken in $CH_3CN$ in the range 200−1100 nm region, CV of L1, UV−vis traces during coulometric oxidation of **7**. X-ray crystallographic data (CCDC number: 865967, 865969, 865966, 865965, 865964, and 865968 for **1**, **3**, **4**, **5**, **6**, and **7**, respectively). This material is available free of charge via the Internet at http://pubs.acs.org.

## ■ AUTHOR INFORMATION

### Corresponding Author

*Email: apurba.patra.nitdgp@gmail.com.

### Notes

The authors declare no competing financial interest.

## ■ ACKNOWLEDGMENTS

Financial support from the Department of Science and Technology (DST), Government of India, (SR/S1/IC-35/2007) is gratefully acknowledged. S. Chatterjee acknowledges the support of CSIR for a junior research fellowship. We sincerely acknowledge the AvH Foundation, Germany, for the equipment donation grant to procure the CHI-1120A spectroelectrochemical analyzer.

## ■ REFERENCES

(1) (a) Review article by Ragsdale, S. W. *J. Biol. Chem.* **2009**, *284*, 18571. (b) Ermler, U.; Grabarse, W.; Shima, S.; Goubeaud, M.; Thauer, R. K. *Curr. Opin. Struct. Biol.* **1998**, *8*, 749.

(2) (a) Vignais, P. M.; Billoud, B. *Chem. Rev.* **2007**, *107*, 4206. (b) Fontecilla-Camps, J. C.; Volbeda, A.; Cavazza, C.; Nicolet, Y. *Chem. Rev.* **2007**, *107*, 4273.

(3) (a) Baidya, N.; Olmstead, M. M.; Mascharak, P. K. *Inorg. Chem.* **1991**, *30*, 929. (b) Colpas, G. J.; Maroney, M. J.; Bagyinka, C.; Kumar, M.; Willis, W. S.; Suib, S. L.; Baidya, N.; Mascharak, P. K. *Inorg. Chem.* **1991**, *30*, 920. (c) Baidya, N.; Olmstead, M. M.; Mascharak, P. K. *J. Am. Chem. Soc.* **1992**, *114*, 9666. (d) Baidya, N.; Olmstead, M. M.; Whitehead, J. P.; Bagyinka, C.; Maroney, M. J.; Mascharak, P. K. *Inorg. Chem.* **1992**, *31*, 3612. (e) Marganian, C. A.; Vazir, H.; Baidya, N.; Olmstead, M. M.; Mascharak, P. K. *J. Am. Chem. Soc.* **1995**, *117*, 1584.

(4) (a) Singh, A. K.; Mukherjee, R. *Dalton Trans.* **2005**, 2886. (b) Patra, A. K.; Mukherjee, R. *Inorg. Chem.* **1999**, *38*, 1388. (c) Mathrubootham, V.; Thomas, J.; Staples, R.; McCraken, J.; Shearer, J.; Hegg, E. L. *Inorg. Chem.* **2010**, *49*, 5393. (d) Bossu, F. P.; Margerum, D. W. *J. Am. Chem. Soc.* **1976**, *98*, 4003. (e) Bossu, F. P.; Margerum, D. W. *Inorg. Chem.* **1977**, *16*, 1210. (f) Lappin, A. G.; Murray, C. K.; Margerum, D. W. *Inorg. Chem.* **1978**, *17*, 1630. (g) Jacobs, S. A.; Margerum, D. W. *Inorg. Chem.* **1984**, *23*, 1195. (h) Sugiura, Y.; Mino, Y. *Inorg. Chem.* **1979**, *18*, 1336. (i) Collins, T. J.; Nichols, T. N.; Uffelman, E. S. *J. Am. Chem. Soc.* **1991**, *113*, 4708. (j) Kruger, H. J.; Peng, G.; Holm, R. H. *Inorg. Chem.* **1991**, *30*, 734. (k) Sunatsuki, Y.; Matsumoto, T.; Fukushima, Y.; Mimura, M.; Hirohata, M.; Matsumoto, N.; Kai, F. *Polyhedron* **1998**, *17*, 1943.

(5) (a) Nag, K.; Chakravorty, A. *Coord. Chem. Rev.* **1980**, *33*, 87. (b) Lappin, A. G.; McAuley, A. *Adv. Inorg. Chem.* **1988**, *32*, 241. (c) Pramanik, K.; Karmakar, S.; Choudhury, S. B.; Chakravorty, A. *Inorg. Chem.* **1997**, *36*, 3562. (d) Haines, R. I.; McAuley, A. *Coord. Chem. Rev.* **1981**, *39*, 77. (e) Baucom, E. I.; Drago, R. S. *J. Am. Chem. Soc.* **1971**, *93*, 6469. (f) Sproul, G.; Stucky, G. D. *Inorg. Chem.* **1973**, *12*, 2898. (g) Panda, R. K.; Acharya, S.; Neogi, G.; Ramaswamy, D. *J. Chem. Soc., Dalton Trans.* **1983**, 1225. (h) Bemtgen, J.-M.; Gimpert, H.-R.; von Zelewsky, A. *Inorg. Chem.* **1983**, *22*, 3576. (i) Mandal, S.; Gould, E. S. *Inorg. Chem.* **1995**, *34*, 3993. (j) Laranjeira, M. C. M.; Marussak, R. A.; Lappin, A. G. *Inorg. Chim. Acta* **2000**, *300*−*302*, 186.

(6) (a) James, T. L.; Cai, L.; Muetterties, M. C.; Holm, R. H. *Inorg. Chem.* **1996**, *35*, 4148. (b) Stavropoulos, P.; Muetterties, M. C.; Carrie, M.; Holm, R. H. *J. Am. Chem. Soc.* **1991**, *113*, 8485. (c) Signor, L.; Knuppe, C.; Hug, R.; Schweizer, B.; Pfaltz, A.; Jaun, B. *Chem.—Eur. J.* **2000**, *6*, 3508. (d) Fox, S.; Stribrany, R. T.; Potenza, J. A.; Schugar, H. J. *Inorg. Chim. Acta* **2001**, *316*, 122. (e) Bhattacharyya, S.; Weakley, T. J. R.; Chaudhury, M. *Inorg. Chem.* **1999**, *38*, 633. (f) Halcrow, M. A.; Christou, G. *Chem. Rev.* **1994**, *94*, 2421. (g) Ge, P.; Riordan, C. G.; Yap, G. P. A.; Rheingold, A. L. *Inorg. Chem.* **1996**, *35*, 5408. (h) Pavlishchuk, V. V.; Kolotilov, S. V.; Sinn, E.; Prushan, M. J.; Addison, A. W. *Inorg. Chim. Acta* **1998**, *278*, 217.

(7) (a) Muresan, N.; Chlopek, K.; Weyhermüller, T.; Neese, F.; Wieghardt, K. *Inorg. Chem.* **2007**, *46*, 5327. (b) Kadish, K. M.; Franzen, M. M.; Han, B. C.; Araullo-McAdams, C.; Sazou, D. *J. Am. Chem. Soc.* **1991**, *113*, 512.

(8) (a) Hartman, J. R.; Vachet, R. W.; Callahan, J. H. *Inorg. Chim. Acta* **2000**, *297*, 79. (b) Phillip, A. T.; Casey, A. T.; Thompson, C. R. *Aust. J. Chem.* **1970**, *23*, 491. (c) Hoskins, B. F.; Whillans, F. D. *J. Chem. Soc., Dalton Trans.* **1975**, 657. (d) Sacconi, L.; Mani, F.; Bencini, A. In *Comprehensive Coordination Chemistry*; Wilkinson, G., Gillard, R. D., McCleverty, J. A., Eds.; Pergamon Press: New York, 1987; Vol. *5*, p 86.

(9) Kryatov, S. V.; Mohanraj, B. S.; Tarasov, V. V.; Kryatov, O. P.; Rybak-Akimova, E. V. *Inorg. Chem.* **2002**, *41*, 923.

(10) (a) Lobana, T. S.; Kumari, P.; Hundal, G.; Butcher, R. J. *Polyhedron* **2010**, *29*, 1130. and references therein. (b) Pedrido, R.; Gonzaléz-Noya, A. M.; Romero, M. J.; Martínez-Calvo, M.; López, M. V.; Gómez-Forneas, E.; Zaragoza, G.; Bermejo, M. R. *Dalton Trans.* **2008**, 6776. (c) Manoj, E.; Kurup, M. R. P. *Polyhedron* **2008**, *27*, 275. (d) Suni, V.; Kurup, M. R. P.; Nethaji, M. *Polyhedron* **2007**, *26*, 3097. (e) Li, M.; Sun, Q.; Bai, Y.; Duan, C.; Zhang, B.; Meng, Q. *Dalton Trans.* **2006**, 2572. (f) Rodríguez-Argüelles, M. C.; López-Silva, E. C.; Sanmartín, J.; Bachhi, A.; Pelizzi, C.; Zani, F. *Inorg. Chim. Acta* **2004**, *357*, 2543. (g) Beshir, A. B.; Guchhait, S. K.; Gascón, J. A.; Fentiani, G. *Bioorg. Med. Chem. Lett.* **2008**, *18*, 498. (h) Roy, S.; Mandal, T. N.; Barik, A. K.; Pal, S.; Gupta, S.; Hazra, A.; Butcher, R. J.; Hunter, A. D.; Zeller, M.; Kar, S. K. *Polyhedron* **2007**, *26*, 2603. (i) Salem, N. M. H.; El-Sayed, L.; Iskander, M. F. *Polyhedron* **2008**, *27*, 3215.

(11) (a) Mahamadou, A.; Jubert, C.; Gruber, N.; Barbier, J.-P. *Eur. J. Inorg. Chem.* **2004**, 1285. (b) Gilbert, J. G.; Addison, A. W.; Butcher, R. J. *Inorg. Chim. Acta* **2000**, *308*, 22. (c) Meyer, F.; Demeshko, S.; Leibeling, G.; Kersting, B.; Kaifer, E.; Pritzkow, H. *Chem.—Eur. J.*

**2005**, *11*, 1518. (d) Chak, B. C. M.; McAuley, A. *Can. J. Chem.* **2006**, *84*, 187. (e) Grapperhaus, C. A.; Kreso, M.; Burkhardt, G. A.; Roddy, J. V. F.; Mashuta, M. S. *Inorg. Chim. Acta* **2005**, *358*, 123. (f) Pandiyan, T.; Barreiro, C. S. S.; jayanthi, N. *J. Coord. Chem.* **2002**, *55*, 1373. (g) Meyer, F.; Kircher, P.; Pritzkow, H. *Chem. Commun.* **2003**, 774. (h) Pavlishchuk, V. V.; Kolotilov, S. V.; Addison, A. W.; Prushan, M. J.; Butcher, R. J.; Thompson, L. K. *Chem. Commun.* **2002**, 468. (i) Chandra, S.; Kumar, R. *Spectrochim. Acta, Part A* **2005**, *62*, 518. (j) Pavlishchuk, V. V.; Kolotilov, S. V.; Addison, A. W.; Butcher, R. J.; Sinn, E. *Dalton Trans.* **2000**, 335. (k) Nandi, S.; Banerjee, D.; Wu, J.-S.; Lu, T.-H.; Slawin, A. M. Z.; Woolins, J. D.; Ribas, J.; Sinha, C. *Eur. J. Inorg. Chem.* **2009**, 3972.

(12) Roy, S.; Mitra, P.; Patra, A. K. *Inorg. Chim. Acta* **2011**, *370*, 247.

(13) *Apex2*; Bruker AXS: Madison, WI, 2006.

(14) Sheldrick, G. M. *Acta Crystallogr., Sect. A* **2008**, *64*, 112.

(15) L. Farrugia, J. *J. Appl. Crystallogr.* **1999**, *32*, 837.

(16) Farrugia, L. J. ORTEP3 for Windows. *J. Appl. Crystallogr.* **1997**, *30*, 565.

(17) Nakamoto, K. *Infrared and Raman Spectra of Inorganic and Coordination Compounds*, 2nd ed.; Wiley: New York, 1970.

(18) Geary, W. J. *Coord. Chem. Rev.* **1971**, *7*, 81.

(19) Murray, S. G.; Hartley, F. R. *Chem. Rev.* **1981**, *81*, 365.

(20) Sellman, D.; Neuner, H. P.; Knoch, F. *Inorg. Chim. Acta* **1991**, *190*, 61.

(21) Rosen, W.; Busch, D. H. *Inorg. Chem.* **1970**, *9*, 262.

(22) (a) Lever, A. B. P. *Inorganic Electronic Spectroscopy*, 2nd ed.; Elsevier: Amsterdam, Oxford, New York, Tokyo, 1984; p 126. (b) Lever, A. B. P. *Inorganic Electronic Spectroscopy*, 2nd ed.; Elsevier: Amsterdam, Oxford, New York, Tokyo, 1984; p 517.

(23) Roy, S.; Javed, S.; Olmstead, M. M.; Patra, A. K. *Dalton Trans.* **2011**, *40*, 12866.

(24) (a) Cooper, S. R.; Rawle, S. C.; Hartman, J. A. R.; Hintsa, E. J.; Adams, G. A. *Inorg. Chem.* **1988**, *27*, 1209. (b) Kettle, S. F. A. *Physical Inorganic Chemistry: A Coordination Chemistry Approach*; Oxford University Press: Oxford, 1998; p 163.

(25) Calculating from the equations: $B = (2\nu_1^2 + \nu_2^2 - 3\nu_1\nu_2)/(15\nu_2 - 27\nu_1)$; for free ion $B$ = 1082 $cm^{-1}$, $\nu = B_{compound}/B_{free\ ion}$; $^3A_{2g} \rightarrow {}^3T_{2g}(F)(\nu_1)$ and $^3A_{2g} \rightarrow {}^3T_{1g}(F)(\nu_2)$.



dx.doi.org/10.1021/ic300606g | *Inorg. Chem.* 2012, 51, 7625−7635